Reptation of active entangled polymers

Andrés R. Tejedor and Jorge Ramírez*

Department of Chemical Engineering, Universidad Politécnica de Madrid, José Gutiérrez Abascal 2, 28006, Madrid, Spain

E-mail: jorge.ramirez@upm.es

Abstract

The dynamical response of entangled polymers can be understood in the framework of the tube theory. In this paper, the dynamics of linear entangled polymers that reptate under the additional action of a drift along the primitive path, are explored. A modified reptation model with drift, valid for small drift values, is presented and solved analytically, as well as by means of Brownian dynamics simulations. When the drift mechanism dominates over diffusion, the transport properties of these active entangled chains change dramatically with respect to the pure reptation case: the viscosity grows linearly with the molecular weight whereas the self-diffusion coefficient becomes independent of the molecular weight. Some open questions regarding possible ways to generate a drift such as the one described are discussed briefly.

The reptation model is the most successful theory to describe the dynamical response of entangled polymers. Originally conceived by de Gennes[1] and later developed by Doi and Edwards,[2–4] the theory has undergone many modifications, such as contour length fluctuations (CLF),[5] tube dilation/dilution,[6,7] or constraint release (CR),[8] in order to describe the linear[9] and non-linear behaviour of branched and polydisperse polymer melts and solutions, as well as complex mixtures of the above.[10]

One of the aspects of the tube theory that has not been explored yet is the response of a system of entangled polymers in the presence of some internal activity. Some recent works have studied the dynamics of active linear[11] [12], semiflexible[13] and ring[14] polymers in dilute solutions and also pasive semiflexible polymers in the presence of an active solvent.[15] In contrast with the above systems, here we consider melts and concentrated solutions of entangled polymers that are propelled along the tube by the action of some internal activity that keeps the system isotropic at all times.

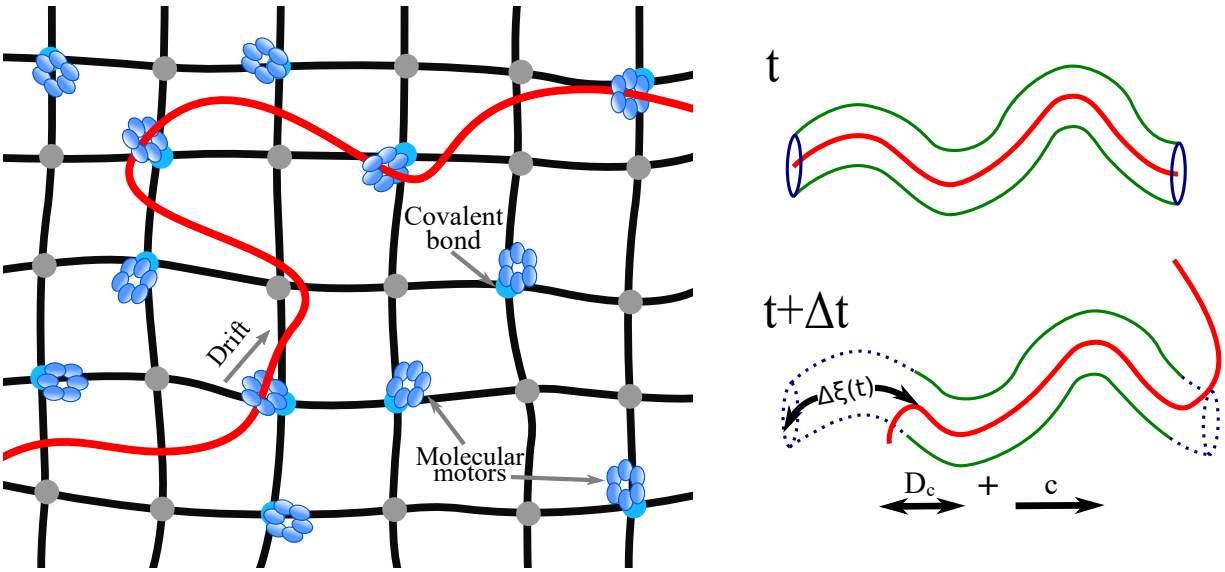

Figure 1: Schematic pictures of: (left) a linear polymer chain moving through a cross-linked network that contains molecular motors covalently attached to the junctions; (right) a chain that reptates with additional drift along the primitive path of the tube at times t (above) and $t + \Delta t$ (below).

Molecular motors represent a possible approach to obtain the proposed mechanism of motion experimentally. In the framework of biology, we can find several examples of active proteins (kinesin, myosin, helicases) that can move in a certain direction along different macromolecules (microtubules, actin, DNA). For example, helicase, an enzyme that helps during the replication of double-stranded DNA, has been shown to move unidirectionally along single-stranded DNA.[16,17] We could take advantage of this type of interaction to generate drift. We envision the following hypothetical case: a linear polymer chain diffusing through a gel of cross-linked polymers (of a different nature to the probe, see Figure 1). The

mesh contains molecular motors homogeneously distributed across the network, covalently attached to all or some of the cross-link points or entanglements. The molecular motors, which have affinity for the sequence of monomers along the probe, can attach to the backbone of the chain, and walk from head to tail, promoting the biased reptation of the probe chain through the mesh from tail to head. The force exerted by the motors on the chain is proportional to the number of entanglements of the probe ($F_T \propto ZF_{\text{motor}}$, where F_{motor} is the force exerted by a single motor on the chain) and therefore to the molecular weight of the chain. The total friction of the polymer moving along the tube is also proportional to the molecular weight ($\zeta_T \propto Z\zeta_{\text{ent}}$, where ζ_{ent} is the friction of a chain strand between entanglements). As a result, the chain will move with a drift velocity that is independent of the chain length, i.e. $c = F_T/\zeta_T = F_{\text{motor}}/\zeta_{\text{ent}}$.

A similar mechanism has been studied in the context of electrophoresis,[18–22] where entangled linear charged polymers move through a gel under the action of an external electric field. However, in the latter, the field induces a preferential direction that breaks the isotropy and the molecules move in the steady state with a constant velocity in the direction of the field, with a mobility that depends on molecular weight.

In this work, we elucidate the impact of a drift velocity that acts along the primitive path axis over the dynamics of a linear entangled polymer chains. Such drift could be the result of some internal activity or a conformational asymmetry of the chain along its contour that favours reptation in one direction over the other. Constraint release is not considered, and thus the model represents the motion of an active entangled chain through a mesh of fixed obstacles. First, we do some basic scaling analysis of the problem, then we calculate the tube segment survival function and the mean square displacement of monomers, comparing the results with the original work of Doi and Edwards,[23] and finally we introduce CLF and verify the main results of the analytical theory by means of Brownian Dynamics Simulations.

In pure reptation theory, the length of the tube L and the friction of the diffusive motion are proportional to the degree of polymerization N, and thus the disengagement time is

proportional to $\tau_d \propto N^2/D_c \propto N^3$, where D_c is the one-dimensional diffusion coefficient of the reptation motion. Since the viscosity is dominated by the slowest relaxation mode, $\eta \propto \tau_d$, it is also proportional to the cube of the molecular weight. Concerning diffusion, every time a molecule escapes from the tube, it diffuses a distance of the order of its own size $\langle R^2 \rangle \propto N$, and therefore $D_G \propto \langle R^2 \rangle / \tau_d \propto N^{-2}$.[24] If we introduce a drift of magnitude c that always acts in the same direction along the primitive path, the characteristic time to escape the tube by this mode of motion is $\tau_c \sim L/c$. For the drift to dominate over reptation $\tau_c \ll \tau_d$, and thus $c \gg 1/N^2$. Typically, in entangled polymers N is a very large number, which sets a very small lower limit for c. Consequently, no matter how small the drift c is, there will always be a sufficiently long linear chain whose dynamics will be governed by it. However, in mildly entangled systems, c must be larger and it might be more difficult to observe the effect of the drift. The change in the terminal time when the drift dominates the relaxation also affects the viscosity and self-diffusion coefficient. If we could envision a material uniquely composed of this type of active entangled chains, discarding any CR effects, its viscosity would scale with N instead of N^3, which would yield materials that are easier to process. Regarding diffusion, since both the chain size and the terminal time are proportional to N, the diffusion coefficient would be independent of the molecular weight, enhancing mass transport significantly. In the following we present the full analytical solution that confirms both results obtained from scaling arguments.

As we want to stick to the original work of de Gennes[1] and Doi and Edwards,[23] we consider a primitive path that is isotropic and has Gaussian statistics at long distances. As a consequence, when the chain ends exit the tube, they must be capable of exploring all possible orientations. This is only possible if the typical time for the chain to move by drift a distance of the order of the tube diameter a is much longer than the Rouse time of one entanglement τ_e, *i.e.* $c \ll a/\tau_e$. If we set the units of length and time as a and τ_e, respectively, this condition changes to $c \ll 1$. With this choice of units, we can express the diffusion coefficient along the primitive path as $D_c = 1/3Z\pi^2$, the Rouse time of the chain

as $\tau_R = Z^2\tau_e = Z^2$, the terminal time $\tau_d = 3Z^3\tau_e = 3Z^3$ and the tube length is $L = Za = Z$, where Z is the number of entanglements.

Following the derivations for pure reptation,[23] we assume that any tube segment that is visited by any of the chain ends is destroyed and We can define the function $\Psi(\xi, t; s)$ as the probability that the chain travels a distance ξ while its ends have not reached the segment s of the initial tube. Taking into account reptation and the drift, the partial differential equation for $\Psi(\xi, t; s)$ is

$$\frac{\partial \Psi}{\partial t} + c\frac{\partial \Psi}{\partial \xi} = D_c \frac{\partial^2 \Psi}{\partial \xi^2}. \tag{1}$$

Given that the tube remains Gaussian, the initial condition is not affected by the drift, *i.e.* $\Psi(\xi, 0; s) = \delta(\xi)$. Since the drift is small, the chain ends can freely explore all possible orientations, and thus the boundary conditions from the original theory are still valid, *i.e.* $\Psi(\xi, t; s)|_{\xi=s} = \Psi(\xi, t; s)|_{\xi=s-Z} = 0$. The solution to the problem above (detailed in the Supplementary Information) gives:

$$\Psi(\xi, t; s) = \frac{2}{Z} \exp\left(\frac{c\xi}{2D_c}\right) \exp\left(\frac{-c^2 t}{4D_c}\right) \sum_{p=1}^{\infty} \sin\left(\frac{p\pi s}{Z}\right) \sin\left(\frac{p\pi(s-\xi)}{Z}\right) \exp\left(-\frac{p^2 t}{\tau_d}\right). \tag{2}$$

From Eq. (2), we can compute the tube segment survival function $\psi(s, t)$ (the probability that the original segment s remains alive after time t) as the integral of $\Psi(\xi, t; s)$ when ξ changes between $s - Z$ and s:

$$\psi(s, t) = 8D_c^2 \pi \exp\left(\frac{cs}{2D_c}\right) \exp\left(\frac{-c^2 t}{4D_c}\right) \sum_{p=1}^{\infty} \sin\left(\frac{p\pi s}{Z}\right) e^{-\frac{p^2 t}{\tau_d}} \frac{p\left[1 - (-1)^p \exp\left(\frac{-cZ}{2D_c}\right)\right]}{4D_c^2\pi^2 p^2 + Z^2 c^2}. \tag{3}$$

In comparison with pure reptation, $\psi(s, t)$ is significantly modified when the drift is introduced: first, the solution of $\psi(s, t)$ loses the head-tail symmetry, which is reflected the exponential dependence on s; second, the sum in Eq. (3) runs over all integers p, and not only odd indices as in pure reptation. As expected, both solutions agree in the limit of zero drift.

As can be seen in Eq. (3), if the time and the length are measured in units of τ_d and Z, respectively, the behaviour of $\psi(s,t)$ is the same when the product cZ^2 is kept constant, as previously predicted by the scaling analysis. In Fig. 2, some snapshots of the evolution of the tube segment survival function are shown for drifts values $cZ^2 = 0$ (pure reptation), 4^{-2}, 4^{-1}, and 4^0 (dominated by the drift), measured at times $t = 0.05\tau_d$ and $0.5\tau_d$. It confirms that the pure reptation solution is restored when the drift vanishes whereas $\psi(s,t)$ gets progressively more asymmetric as c increases. We can also observe a sharper decay of the tube segment survival function at the head of the chain (s values close to Z). As the chain is being pushed towards the head, the tube segments closer to the tail of the tube are destroyed faster. At very short times ($t \ll \tau_c$, dotted lines), the dynamics of the chain is governed by diffusion (displacement $\propto t^{0.5}$) over drift ($\propto t$) even for significant drifts ($cZ^2 = 4^{-1}$). At $t = \tau_d/2$ (solid lines) the drift is the dominant mechanism of relaxation for large enough values of the drift (approximately $cZ^2 > 4^{-1}$).

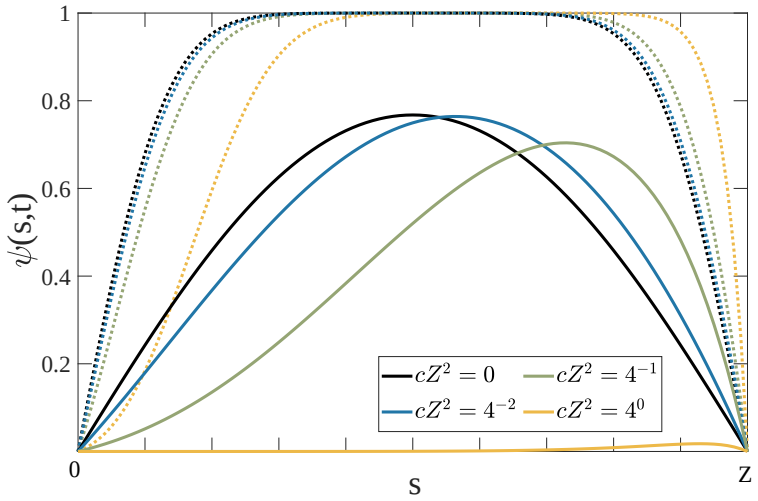

Figure 2: Evolution of the tube segment survival function $\psi(s,t)$ (Eq. (3)) for pure reptation $c = 0$ and for increasing values of the drift velocity $cZ^2 = 4^{-2}$, 4^{-1} and 4^0. The function is plotted for $t = 0.05\tau_d$ (dotted lines) and $t = 0.5\tau_d$ (solid lines).

The convergence of the analytical solution fails when the drift exceeds $cZ^2 \simeq 1$ even if a large number of modes is used in the sum. This numerical limit is tighter than the physical limit $c \ll 1$ discussed above and restricts the range of c values that can be handled

analytically. However, as shown in Fig. 2, this range is wide enough to explore and quantify the effects of drift. This numerical limit does not affect the physics of the problem, which can be studied by means of simulations.

Using $\psi(s,t)$, we can derive the tube survival function $\psi(t)$, defined as the fraction of the original tube that is still alive at time t:

$$\psi(t) = \frac{1}{Z}\int_0^Z ds\,\psi(s,t) = 8D_c^4\pi^2 \exp\left(\frac{-c^2 t}{4D_c}\right)\sum_{p=1}^{\infty} e^{-\frac{p^2 t}{\tau_d}} \frac{8p^2\left[1-(-1)^p\cosh\left(\frac{cZ}{2D_c}\right)\right]}{(4D_c^2\pi^2p^2+c^2Z^2)^2}. \qquad (4)$$

Again, the pure reptation solution[23] is recovered when the drift vanishes. In Fig. 3 we plot the solution of Eq. (4) for the same values of c used before (solid lines). It shows how the terminal time decreases and the terminal region becomes sharper as the drift velocity becomes larger (see $cZ^2 = 4^0$). As the value of c increases, the terminal time transitions smoothly from τ_d to τ_c.

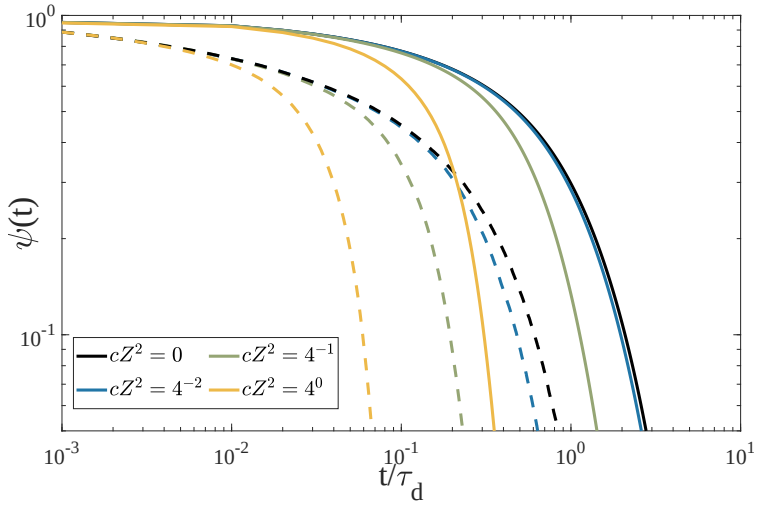

Figure 3: Tube survival function with CLF $\psi^{\mathrm{CLF}}(t)$ (dashed lines, for $Z = 8$ and $N_s = 4$) and without CLF $\psi(t)$ (solid lines, Eq. (4), for increasing values of the drift $cZ^2_{\mathrm{eff}}, cZ^2 = 0, 4^{-2}$, 4^{-1} and 4^0).

From the tube survival function we can compute the relaxation modulus as $G(t) = G_0\psi(t)$, where the plateau modulus G_0 is a property of the particular polymer under study.[25] From the relaxation modulus $G(t)$ we can extract the viscosity as $\eta = G_0\int_0^\infty dt\,\psi(t)$, and

hence:

$$\eta = 256 G_0 D_c^6 \pi^4 \tau_d \sum_{p=1}^{\infty} \frac{p^2 \left[1 - (-1)^p \cosh\left(\frac{cZ}{2D_c}\right)\right]}{(4D_c^2\pi^2 p^2 + c^2 Z^2)^3}. \tag{5}$$

The drift governs the value of the viscosity when $\cosh(cZ/2D_c) \gg 1$. In this limit, the asymptotic value of the viscosity can be calculated from Eq. (5) to give $\eta_\infty = ZG_0/2c$, which exhibits a linear dependence with respect to the molecular weight, whereas in the pure reptation limit the scaling is cubic. This is in agreement with our previous scaling argument.

It is interesting to explore if contour length fluctuations affect the obtained results. Since the problem of reptation with CLF cannot be solved analytically, we run simulations of a molecular model of the tube theory that respects the description given by Doi and Edwards[23] and that has been used previously by other groups.[26] In the model, a one-dimensional Rouse chain diffuses along the primitive path, represented by a three-dimensional random walk of step length a, while a tension $3k_BT/a$ is pulling from both ends. We discretize the chain in $N = ZN_e$ harmonic springs and define the current length tube by locating the position of the end beads. In this model, the tube limit is reached when $N_e \to \infty$. By action of the fluctuations, the effective number of entanglements is reduced as $Z_{\text{eff}} = Z(1 - X/\sqrt{Z})$ where X=1.47.[5] Thus, we expect that, in the presence of drift, the previously obtained analytical results will still hold when the product cZ_{eff}^2 is kept constant.

In Fig. 3 we plot $\psi^{\text{CLF}}(t)/Z$ (dashed lines) for a system with $Z = 8$, $N_e = 4$ and drift velocities $cZ_{\text{eff}}^2 = 0, 4^{-2}, 4^{-1}, 4^0$. As in the analytical solution, a large drift accelerates the escape from the tube and sharpens the decay in the terminal region. It can also be seen that CLF is very effective at destroying tube segments close to the ends at early times, even when the drift is introduced. In contrast, at long times the drift has a non-trivial effect whether CLF is present or not. For example, for small drifts, *i.e.* comparing the cases for $c = 0$ and $cZ_{\text{eff}}^2 = 4^{-2}$, it can be observed that the drift is more effective at destroying the tube in the CLF case than in pure reptation (the distance between the dashed lines is larger than between the solid lines). However, for larger drifts, *i.e.* if we compare the curves for

$cZ_{\text{eff}}^2 = 4^{-1}$ and $cZ_{\text{eff}}^2 = 4^0$, we can see that the drift accelerates the relaxation of the tube more in the pure reptation case than in the CLF case (the distance between the dashed lines is smaller than between the solid lines). There seem to be a cooperative effect between CLF and the drift that enhances the relaxation of the tube at small values of c but is not effective at large c values.

It is also interesting to study the segmental motion of the monomers. As in the work of Doi and Edwards,[23] we start by calculating the general function $\phi(s, s'; t) = \langle(\mathbf{R}(s,t) - \mathbf{R}(s',0))^2\rangle$. By formulating a stochastic differential equation for $\mathbf{R}$ we can derive the following partial differential equation for $\phi(s, s'; t)$ (see the Supplementary Information for details):

$$\frac{\partial \phi}{\partial t} - c\frac{\partial \phi}{\partial s} = D_c \frac{\partial^2 \phi}{\partial s^2}. \tag{6}$$

Note that the sign of the drift term changes with respect to Eq. (1). Again, we keep the initial and boundary conditions from pure reptation, *i.e.* is $\phi(s, s'; 0) = |s - s'|$, and $\partial_s \phi(s, s'; t)|_{s=Z} = 1$, $\partial_s \phi(s, s'; t)|_{s=0} = -1$. Computing the solution for this problem and setting $s' = s$, the mean square displacement (MSD) $g_1(s, t)$ of the segment s is readily obtained:

$$g_1(s,t) = ct \coth\left(\frac{cZ}{2D_c}\right) + \sum_{p=1}^{\infty} \frac{(1 - e^{-D_c \lambda_p^2 t}) 16 D_c^2 Z}{4D_c^2 p^2 \pi^2 + c^2 Z^2} \left[\cos^2\left(\frac{p\pi s}{Z}\right) - \frac{c^2 Z^2}{4D_c^2 p^2 \pi^2 + c^2 Z^2}\right], \tag{7}$$

where $\lambda_p^2 = c^2/4D_c^2 + p^2\pi^2/Z^2$. By inspecting Eq. (7), we can observe that $g_1(s, t)$ still exhibits a head-tail symmetry which is independent of the drift. Again, measuring the time in units of τ_d, it can be observed that $g_1(s, t)/Z$ does not depend on Z when keeping the product cZ^2 constant. In Fig. 4, $g_1(s, t)/Z$ of the central monomer ($s = Z/2$) is shown for the same values of the drift velocity c used previously (dashed lines), where the pure reptation solution is again recovered in the limit of very small drifts. The expected power laws from reptation are observed, *i.e.* $g_1(s, t) \propto t^{0.5}$ when $t \ll \tau_d$ and $g_1(s, t) \propto t$ when $t \gg \tau_d$, but the transition to the terminal Fickian regime occurs earlier as the drift c increases.

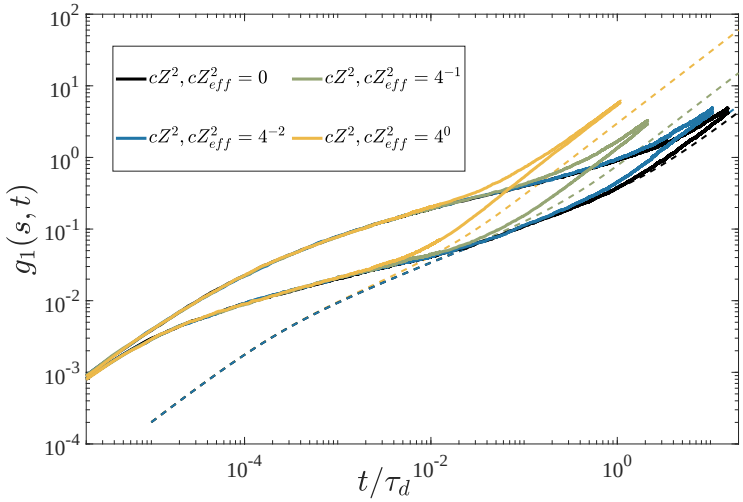

Figure 4: Mean square displacement of monomers divided by Z from: simulations of reptating chains with CLF (solid lines, $Z = 32$ and $N_e = 2$, $s = 0, Z/2$) and analytical solutions of pure reptation, Eq. (7) (dashed line, $s = Z/2$) for different values of drift cZ^2_{eff}, $cZ^2 = 0, 4^{-2}, 4^{-1}, 4^0$.

From the long-time limit of Eq. (7), where the dominant term is the hyperbolic cosine, we can extract the diffusion coefficient:

$$D_G = \lim_{t\to\infty} \frac{g_1(s,t)}{6t} = \frac{c}{6} \coth\left(\frac{cZ}{2D_c}\right). \tag{8}$$

Again, in the limit of very small drifts, D_G agrees with the solution for pure reptation.[23] For significant drifts, the diffusion coefficient in Eq. (8) becomes independent of the molecular weight, *i.e.* $D_G \to c/6$, which agrees with the scaling argument previously obtained.

We can also compute the segmental motion from simulations with CLF. In Fig. 4 we plot $g_1(s,t)$ with CLF for the central and one of the end monomers. For small drifts, the famous four power laws for g_1 of the central monomer are recovered.[23] In contrast, as the drift increases, the time necessary to escape the tube is reduced and the the transition to the terminal Fickian time appears earlier. This transition can occur between τ_R and τ_d (see $cZ^2_{\text{eff}} = 4^{-2}$ and $cZ^2_{\text{eff}} = 4^{-1}$) or between τ_e and τ_R (see the fastest drift value in Fig. 4). In the latter case, the $t^{0.5}$ scaling that appears in CLF between τ_R and τ_d is completely absent. Note that, as $c \ll a/\tau_e$, the transition to the terminal Fickian regime due to drift can never

emerge before τ_e.

To conclude, we have revisited the original reptation theory, as developed by Doi and Edwards, introducing a drift term in addition to the thermal diffusion. Under the assumptions of our theory, the most relevant results are the following: i) even though the drift c may be small, there will always be a sufficiently long polymer chain for which the drift will be the dominant relaxation mechanism; ii) when entangled active linear chains reptate through a gel and the drift governs, they move by Fickian diffusion and their self-diffusion coefficient is independent of the molecular weight, whereas it decays with N^{-2} in pure reptation ; iii) a melt composed of this type of active linear polymers would have a very low viscosity that grows linearly with N instead of with N^3 (neglecting any constraint release effects). All these results have been derived from scaling arguments, analytical theory and simulations. It remains to find a possible route to introduce drift in real entangled systems. We assume that this could be possible in the framework of active matter, by the action of active colloids or molecular motors that propel the chain in a particular direction along the tube. In addition, we hypothesize that a reptating chain with drift could result from some internal conformational asymmetry that favours reptation in one direction over the other. In conclusion, our results can be used to develop new macromolecular materials with enhanced transport properties (lower viscosity and higher diffusion coefficient) that do not depend so unfavourably on the molecular weight.

Acknowledgements

This work was funded by grants FIS2016-78847-P of the MEC and PEJ-2017-AI/IND-6767 from the Regional Government of Madrid. We acknowledge the computer resources and technical assistance provided by the Centro de Supercomputacion y Visualizacion de Madrid (CeSViMa).

Supporting Information. Detailed analytical solution for the tube segment survival

function and the segmental motion of a reptating chain with drift.

References

(1) de Gennes, P. G. Reptation of a Polymer Chain in the Presence of Fixed Obstacles. *J. Chem. Phys.* **1971**, *55*, 572.

(2) Doi, M.; Edwards, S. Dynamics of concentrated polymer systems. Part 1.Brownian motion in the equilibrium state. *J. Chem. Soc. Faraday Trans. 2* **1978**, *74*, 1789–1801.

(3) Doi, M.; Edwards, S. Dynamics of concentrated polymer systems. Part 2.Molecular motion under flow. *J. Chem. Soc. Faraday Trans. 2* **1978**, *74*, 1802–1817.

(4) Doi, M.; Edwards, S. Dynamics of concentrated polymer systems. Part 3.The constitutive equation. *J. Chem. Soc. Faraday Trans. 2* **1978**, *74*, 1818–1832.

(5) Doi, M. Explanation for the 3.4-power law for viscosity of polymeric liquids on the basis of the tube model. *J. Polym. Sci. B* **1983**, *21*, 667–684.

(6) Marrucci, G. Relaxation by reptation and tube enlargement: A model for polydisperse polymers. *J. Polym. Sci. B* **1985**, *23*, 159–177.

(7) Milner, S. T.; McLeish, T. C. B. Parameter-Free Theory for Stress Relaxation in Star Polymer Melts. *Macromolecules* **1997**, *30*, 2159–2166.

(8) Rubinstein, M.; Colby, R. H. Self-consistent theory of polydisperse entangled polymers: Linear viscoelasticity of binary blends. *J. Chem. Phys.* **1988**, *89*, 5291–5306.

(9) Likhtman, A. E.; McLeish, T. C. Quantitative theory for linear dynamics of linear entangled polymers. *Macromolecules* **2002**, *35*, 6332–6343.

(10) Das, C.; Read, D. J.; Auhl, D.; Kapnistos, M.; den Doelder, J.; Vittorias, I.; McLeish, T. C. Numerical prediction of nonlinear rheology of branched polymer melts. *J. Rheol.* **2014**, *58*, 737–757.

(11) Kaiser, A.; Babel, S.; ten Hagen, B.; von Ferber, C.; Löwen, H. How does a flexible chain of active particles swell? *J. Chem. Phys.* **2015**, *142*, 124905.

(12) Bianco, V.; Locatelli, E.; Malgaretti, P. Globulelike Conformation and Enhanced Diffusion of Active Polymers. *Physical Review Letters* **2018**, *121*.

(13) Ghosh, A.; Gov, N. Dynamics of active semiflexible polymers. *Biophys. J.* **2014**, *107*, 1065–1073.

(14) Mousavi, S. M.; Gompper, G.; Winkler, R. G. Active Brownian ring polymers. *J. Chem. Phys.* **2019**, *150*, 064913.

(15) Harder, J.; Valeriani, C.; Cacciuto, A. Activity-induced collapse and reexpansion of rigid polymers. *Phys. Rev. E* **2014**, *90*, 062312.

(16) Kim, D.-E.; Narayan, M.; Patel, S. S. T7 DNA helicase: a molecular motor that processively and unidirectionally translocates along single-stranded DNA. *Journal of molecular biology* **2002**, *321*, 807–819.

(17) Stano, N. M.; Jeong, Y.-J.; Donmez, I.; Tummalapalli, P.; Levin, M. K.; Patel, S. S. DNA synthesis provides the driving force to accelerate DNA unwinding by a helicase. *Nature* **2005**, *435*, 370.

(18) Slater, G. W.; Noolandi, J. New Biased-Reptation Model For Charged Polymers. *Phys. Rev. Lett.* **1985**, *55*, 1579–1582.

(19) Lumpkin, O. J.; Déjardin, P.; Zimm, B. H. Theory of gel electrophoresis of DNA. *Biopolymers* **1985**, *24*, 1573–1593.

(20) Slater, G. W.; Noolandi, J. On the reptation theory of gel electrophoresis. *Biopolymers* **1986**, *25*, 431–454.

(21) Duke, T.; Viovy, J.-L.; Semenov, A. N. Electrophoretic mobility of DNA in gels. I. New biased reptation theory including fluctuations. *Biopolymers* **1994**, *34*, 239–247.

(22) Viovy, J.-L. Reptation theories of electrophoresis. *Mol. Biotechnol.* **1996**, *6*, 31–46.

(23) Doi, M.; Edwards, S. *The Theory of Polymer Dynamics*; Oxford University Press, 1988; Vol. 73.

(24) De Gennes, P.-G.; Gennes, P.-G. *Scaling concepts in polymer physics*; Cornell university press, 1979.

(25) Larson, R. G.; Sridhar, T.; Leal, L. G.; McKinley, G. H.; Likhtman, A. E.; McLeish, T. C. B. Definitions of entanglement spacing and time constants in the tube model. *J. Rheol.* **2003**, *47*, 809.

(26) Wang, Z.; Larson, R. G. Constraint Release in Entangled Binary Blends of Linear Polymers: A Molecular Dynamics Study. *Macromolecules* **2008**, *41*, 4945–4960.

Graphical TOC Entry